J|A|C|S
COMMUNICATIONS

Published on Web 10/07/2005

One-Dimensional Assembly of Chalcogenide Nanoclusters with Bifunctional Covalent Linkers

Nanfeng Zheng,[†] Xianhui Bu,*[,‡] Haiwei Lu,[†] Lan Chen,[‡] and Pingyun Feng*[,†]

Department of Chemistry, University of California, Riverside, California 92521, and Department of Chemistry and Biochemistry, California State University, 1250 Bellflower Boulevard, Long Beach, California 90840

Received August 14, 2005; E-mail: xbu@csulb.edu; pingyun.feng@ucr.edu

Nanocluster superlattices that are periodic arrays of nanoclusters represent a new class of materials that are different from either individual nanoclusters or condensed solids. The collective properties of nanocrystal superlattices are dependent on both individual clusters and their patterns of organization.[1−3] Compared to two- or three-dimensional assemblies, anisotropic one-dimensional (1D) assemblies are generally more difficult to prepare and require appropriate linear templates or other directional organization forces. Even though different approaches have been developed to achieve various 1D assemblies of nanocrystals, few studies have been done on the assembly of crystallographically well-defined chalcogenide nanoclusters with different organic ligands.[3]

We have now prepared a series of 1D assemblies of chalcogenide nanoclusters in which bifunctional ligands are employed as the directional linker. Single crystal analysis reveals interesting structural isomerization of tetrahedral clusters and different linking modes. It is demonstrated that organic ligands of various length and rigidity can be used for the assembly, making it possible to create organized nanocluster−ligand structures through synthetic design of either nanoclusters or bridging ligands, in addition to various patterns of organization.

These covalent superstructures are denoted as COV-*q*, where *q* is an integer indicating a particular structure type. The *q* is followed by the composition of clusters and names of organic ligands, and sometimes cationic charge-balancing species (e.g., COV-2CdS-TMDPy-TPhP, Table 1). For simplicity, we also use general terms such as Cd-8, Cd-17, and Cd-32 to refer to a nanocluster that contains the specified number of metal cations.

All materials reported here were synthesized under solvothermal conditions between 85 and 150 °C.[4] Cd^{2+} and SPh^- sources are in the form of $Cd(SPh)_2$ or $(NMe_4)_2[Cd_4(SPh)_{10}]$.[5] The S^{2-} source can be either thiourea or $Na_2S_2O_3$. Bifunctional ligands employed here are different types of bipyridines. The solvent can be CH_3CN, H_2O, or a mixture of CH_3CN and H_2O in various ratios.

Chalcogenide nanoclusters reported here are related to a series of tetrahedron-shaped clusters termed capped tetrahedral clusters (denoted as C*n*) and their isomers (denoted as C*n*,*m*, $m = 1-4$) with a different number of corners rotated by 60° from the original position in C*n* clusters.[6,7] Prior to this work, few C*n*,*m* clusters are known, and nearly all C*n* clusters were synthesized in the form of molecular crystals or covalent superlattices through corner-sharing thiolates.[8−12] Few examples of the covalent coassembly between chalcogenide nanoclusters and organic ligands exist.[13]

In 1D assemblies reported here, there are two types of Cd-32 clusters. The Cd-32 cluster in COV-1 ($Cd_{32}S_{14}(SPh)_{36}L_4$, L = terminal pyridyl group) has only one barrelanoid cage rotated (C2,1, Figure 1A). In comparison, the Cd-32 clusters in COV-2 ($Cd_{32}S_{14}(SPh)_{38}L_2^{2-}$) have two corners rotated (C2,2, Figure 1B).

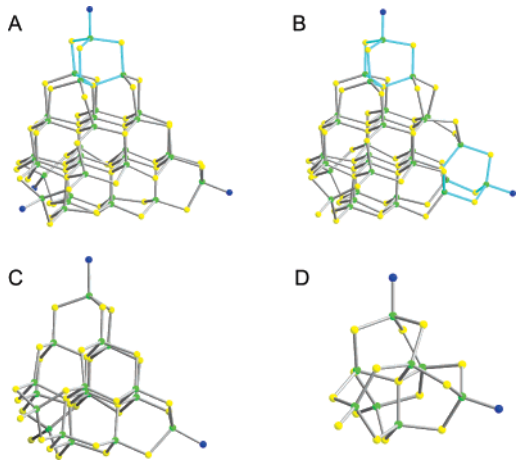

Figure 1. Four geometrically different clusters synthesized in this study. (A) The C2,1 cluster in COV-1 has one corner barrelanoid cage rotated. (B) The C2,2 cluster in COV-2 has two corner cages rotated. The rotated cages are highlighted in cyan. (C) The C1 cluster in COV-3. (D) The C0 cluster in COV-4. Green, Cd^{2+}; yellow, S; blue, nitrogen in the pyridyl group. Carbons in −SPh and bridging bipyridines are omitted for clarify.

In addition to C2,1 and C2,2 clusters, other clusters such as Cd-17 (C1, Figure 1C) and Cd-8 (C0 or P1, Figure 1D) have also been synthesized as building blocks for different 1D assemblies.[7a]

For 1D assemblies of Cd-32 clusters, two linking modes in which either four or two corners are used for cross-linking have been observed. In COV-1, adjacent C2,1 CdS clusters are joined together through two TMDPy ligands into a doubly bridged chain (Figure 2A). The replacement of all four corner −SPh groups by neutral ligands results in neutral chains (and clusters) that are aligned in the same direction and packed together through noncovalent interactions. In comparison, adjacent C2,2 CdS clusters in COV-2 are joined together through only one TMDPy molecule into singly bridged chains (Figure 2B). The replacement of only two −SPh corners by neutral ligands decreases the charge on each Cd-32 cluster from −4 to −2. The packing of these negative chains must therefore leave void space to accommodate charge-balancing cations. Among materials reported here, COV-2 is the only covalent superstructure that contains separate cationic and anionic components.

Similar to Cd-32 clusters, Cd-17 and Cd-8 clusters can also be linked into 1D assemblies. However, Cd-17 and Cd-8 only form singly bridged chains with alternating ligands and nanoclusters. Unlike Cd-32 clusters that can use up to four corners for cross-linking, Cd-17 and Cd-8 clusters use only two corners because of their −2 charge, which explains their preference for the formation of 1D configuration. This linking mode avoids the formation of positively charged cluster−ligand assemblies that may be unfavorable under our synthetic conditions. For Cd-17 clusters in

[†] University of California
[‡] California State University.

10.1021/ja055376x CCC: $30.25

Table 1. A Summary of Crystallographic Data in This Study[a]

name[b]	cluster	cluster composition[c]	space group	*a* (Å)	*b* (Å)	*c* (Å)	*β* (°)	*R*1
COV-1CdS−TMDPy	C2,1 CdS	$Cd_{32}S_{14}(SPh)_{36}L_4$	*C*2/*c*	31.5032(5)	30.1445(5)	61.3699(10)	94.982(1)	7.89%
COV-2CdS-TMDPy-TPhP	C2,2 CdS	$Cd_{32}S_{14}(SPh)_{38}L_2^{2-}$	*Ibca*	26.3539(8)	34.5150(10)	73.258(2)	90	7.77%
COV-3CdS−BPy	C1 CdS	$Cd_{17}S_4(SPh)_{26}L_2$	*C*2/*c*	30.0750(5)	58.6144(10)	31.8999(5)	101.945(1)	5.69%
COV-3CdSeS−BPy	C1 CdSeS	$Cd_{17}Se_4(SPh)_{26}L_2$	*C*2/*c*	30.315(2)	57.374(5)	31.765(3)	100.975(3)	
COV-4CdS-TMDPy	C0 CdS	$Cd_8S(SPh)_{14}L_2$	$P2_1/n$	23.4374(4)	18.9054(3)	24.3535(4)	108.546(1)	4.37%

[a] X-ray data were collected on a Bruker APEX CCD diffractometer with a Mo Kα at 90−150 K. The structures were refined using XShell 6.2. The final full-matrix refinements were against F^2. $R(F) = \sum||Fo| - |Fc||/\sum|Fo|$ with $Fo > 4.0\sigma(F)$. [b] TPhP = tetraphenylphosphonium, $C_{24}H_{20}P^+$; TMDPy = 4,4′-trimethylenedipyridine, $C_{13}H_{14}N_2$; BPy = 4,4′-bipyridine, $C_{13}H_{14}N_2$. [c] L = Pyridyl at the cluster corner. The number of ligand molecules per formula is half of the number of pyridyl groups. [d] Due to disorder of surface-capping phenyl groups, it is not possible to obtain accurate bond lengths involving carbon atoms. Thermal ellipsoids for light atoms, such as carbon, also tend to be elongated or otherwise irregular. In addition, diffraction intensity at high angles is weak for COV-2 ($2\theta_{max} = 40°$), which leads to relatively high *R*(int) of 13.3% and high *wR*2 of 28.8%.

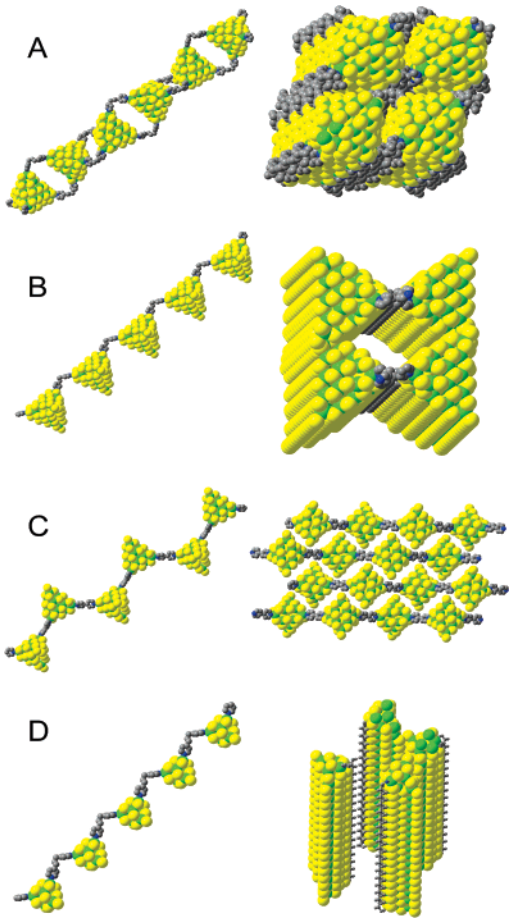

Figure 2. One-dimensional assemblies of CdS clusters. (A) In COV-1, adjacent C2,1 CdS clusters are joined together through two TMDPy molecules into chains. (B) In COV-2, each C2,2 CdS cluster alternates with one TMDPy molecule to form negatively charged chains. (C) In COV-3, C1 CdS or CdSeS clusters are joined by BPy into zigzag chains. (D) In COV-4, C0 $Cd_8S(SPh)_{14}$ clusters are connected into 1D chains through TMDPy ligands. Diagrams at the second column show the 3D packing of chains.

COV-3CdS, rigid 4,4′-bipyridine (BPy) is used (Figure 2C), whereas for Cd-8 clusters in COV-4, flexible TMDPy is used as the bridging ligand (Figure 2D).

With different semiconducting nanoclusters as building blocks, these materials exhibit optical size-dependent properties. The optical absorption of the materials is red-shifted to longer wavelength when larger clusters are used as building blocks. With Cd-8 clusters as the building block, COV-4 CdS-TMDPy exhibits the maximum absorption at 289 nm. In comparison, the maximum absorption of COV-3 CdS−BPy based on Cd-17 clusters is red-shifted to 305 nm. Further red-shift is observed for COV-1 CdS-TMDPy containing Cd-32 clusters ($\lambda_{max} = 335$ nm) (Figure S1). Compared to the solution containing corresponding discrete clusters, solid nanocluster superlattices show broader absorption spectra with the onset of their absorption red-shifted to longer wavelength, which is apparently due to the intercluster interaction within the unique assemblies reported here.[14]

Acknowledgment. We thank the NSF (P.F.), Beckman Foundation (P.F.), and the donors of the Petroleum Research Fund (administered by the ACS) (X.B. and P.F.) for the support of this work. P.Y. is an Alfred P. Sloan research fellow and Camille Dreyfus Teacher-Scholar.

Supporting Information Available: Crystallographic data including positional parameters, thermal parameters, and bond distances and angles (CIF). This material is available free of charge via the Internet at http://pubs.acs.org.

References

(1) Xia, Y.; Yang, P.; Sun, Y.; Wu, Y.; Mayers, B.; Gates, B.; Yin, Y.; Kim, F.; Yan, H. *Adv. Mater.* **2003**, *15*, 353−466.
(2) Tang, Z.; Kotov, N. A. *Adv. Mater.* **2005**, *17*, 951−962.
(3) Schmid, G.; Simon, U. *Chem. Commun.* **2005**, 697−710.
(4) Typical synthesis conditions are given using COV-1 as an example; 47 mg of thiourea, 183 mg of $Cd(SPh)_2$, 45 mg of PPh_4Br, 96 mg of TMDPy, and 2.565 g of CH_3CN were mixed in a 23 mL Teflon-lined stainless steel autoclave and stirred for ∼20 min. The vessel was sealed and heated at 110 °C for 2 days. After cooling to room temperature, pale yellow crystals of COV-1 CdS−TMDPy were obtained.
(5) (a) Dance, I. G.; Garbutt, R. G.; Craig, D. C.; Scudder, M. L. *Inorg. Chem.* **1987**, *26*, 4057−4064. (b) Dance, I. G.; Choy, A.; Scudder, M. L. *J. Am. Chem. Soc.* **1984**, *106*, 6285−6295.
(6) Dance, I. G.; Fisher, K. *Prog. Inorg. Chem.* **1994**, *41*, 637−803.
(7) (a) Feng, P.; Bu, X.; Zheng, N. *Acc. Chem. Res.* **2005**, *38*, 293−303. (b) Zheng, N.; Bu, X.; Lu, H.; Zhang, Q.; Feng, P. *J. Am. Chem. Soc.* **2005**, *127*, 11963−11965.
(8) Lee, G. S. H.; Craig, D. C.; Ma, I.; Scudder, M. L.; Bailey, T. D.; Dance, I. G. *J. Am. Chem. Soc.* **1988**, *110*, 4863−4864.
(9) Herron, N.; Calabrese, J. C.; Farneth, W. E.; Wang, Y. *Science* **1993**, *259*, 1426−1428.
(10) Vossmeyer, T.; Reck, G.; Schulz, B.; Katsikas, L.; Weller, H. *J. Am. Chem. Soc.* **1995**, *117*, 12881−12882.
(11) Behrens, S.; Bettenhausen, M.; Deveson, A. C.; Eichhoefer, A.; Fenske, D.; Lohde, A.; Woggon, U. *Angew. Chem., Int. Ed.* **1996**, *35*, 2215−2218.
(12) Vossmeyer, T.; Reck, G.; Katsikas, L.; Haupt, E. T. K.; Schulz, B.; Weller, H. *Science* **1995**, *267*, 1476−1479.
(13) (a) Zheng, N.; Bu, X.; Feng, P. *J. Am. Chem. Soc.* **2002**, *124*, 9688−9689. (b) Xie, J.; Bu, X.; Zheng, N.; Feng, P. *Chem. Commun.* **2005**, 4916−4918.
(14) Doellefeld, H.; Weller, H.; Eychmueller, A. *J. Phys. Chem. B* **2002**, *106*, 5604−5608.

JA055376X